IJHSR
ijhighschoolresearch.org

■ RESEARCH ARTICLE

Hierarchical Optimal Path Planning (HOPP) for Robotic Apple Harvesting

David W Liu
Athens Academy, 1281 Spartan Ln, Athens, GA, 30606, USA; david.weizhong.liu@gmail.com

ABSTRACT: Apples are among the most consumed fruits in the United States. Currently, almost all apples destined for the fresh market are picked by the human hand. Due to the shortage of seasonal manual labor and rising costs in manual apple picking, robotic apple harvesting has been explored for years. However, a challenge in developing and deploying an apple harvesting robotic system is how to deal with the unstructured apple tree environment. This work aims to demonstrate that structured 3D model representation of apple trees can significantly enable and facilitate robotic apple harvesting, particularly for optimal 3D path planning. Accordingly, a hierarchical optimal path planning (HOPP) algorithm is designed to significantly reduce or minimize the time cost during robotic apple harvesting in a 3D environment. The core idea of this HOPP algorithm is applying distance-constrained k-means clustering to group apples into 3D harvesting zones first, after which an optimal 3D robotic harvesting path is derived via the Traveling Salesman Problem (TSP) formulation and solution. Within each 3D apple harvesting zone, a second-stage optimal path planning is conducted by the TSP method on individual apples. Experiments showed that the proposed HOPP algorithm is promising.

KEYWORDS: Robotics; Agriculture; Apple Harvesting; Path Planning.

■ Introduction

Apples are America's most consumed and favorite fruit and are either eaten raw or consumed in other ways. The American apple industry, with 5,000+ producers, brings billions of dollars to the economy each year and contributes nutritious fruit/food to consumers around the world. Remarkably, the most labor-intensive task in apple production is harvesting, and nearly all apples destined for the fresh market in America are picked by the human hand. Apple growers reported that harvesting labor accounts for approximately a third of their annual variable costs - as much as pruning and thinning combined.[1] In addition, manual apple harvesting is a time-sensitive operation where variable weather patterns generate uncertainty during employment planning and is costly.[1] For example, the threat of an early fall frost could cause a short-term surge in the demand for apple pickers. Also, picking fresh market apples is both physically strenuous and highly repetitive. Apple picking exposes workers to fall hazards as well as ergonomic injuries through heavy lifting and repetitive hand actions. Therefore, to deal with the shortage of seasonal manual labor, rising costs, and risks to workers in manual apple picking, robotic apple harvesting has been explored for decades.[2]

Robotics researchers have been actively working on the development of apple harvesting robots since the 1980s.[2] In this field, visual fruit harvesting robots are common as reviewed recently.[3] Typically, a fruit harvesting robot uses visual sensing, e.g., via 2D cameras, stereo vision systems, laser active vision systems, or multi-spectral imaging technologies, to perceive and learn fruit information such as location, shape, size, color, etc. The main technical tasks of those visual sensing systems include camera calibration, fruit target recognition and positioning, background recognition, 3D fruit reconstruction, and robotic path and trajectory planning. Those visual sensing systems also use visual servocontrol picking mechanisms to perform real fruit harvesting. However, a notable missing piece of those existing visual sensing systems for fruit harvesting is that they are not designed for global 3D mapping or reconstruction of all fruits on the entire tree, e.g., all apples on a tree. Instead, existing visual sensing techniques in robotic fruit harvesting are targeting individual or a few fruits in the local context. The lack of global information of distributions or localizations of all apples on a tree hampers the possibility of global optimal 3D path planning for actual apple harvesting. In response, this study contributes a unique investigation of how much gain can be achieved for optimal 3D path planning in robotic apple harvesting if 3D models of apples and their trees are available, which can stimulate and motivate future innovation in developing 3D reconstruction and mapping approaches for robotic apple harvesting and robotic fruit harvesting in general.

This work is also motivated by a fact that unstructured apple tree environment is a major challenge in developing and deploying apple harvesting robotic systems in real world scenarios, as pointed out and emphasized by literature papers.[1-3] By leveraging an existing realistic 3D model of an apple tree and its hundreds of apples, this work will demonstrate that 3D representation of apples can significantly enable and facilitate robotic apple harvesting, particularly for optimal 3D path planning. Along this direction, a hierarchical optimal path planning (HOPP) algorithm is designed to significantly reduce or minimize the time cost during robotic apple harvesting in a 3D environment. Specifically, the 3D HOPP algorithm is composed of two stages: 1) applying distance-constrained k-means clustering4 to group apples into harvesting zones first, based on which an optimal

DOI: 10.36838/v4i4.6

robotic harvesting path is derived via the Traveling Salesman Problem (TSP) formulation and solution;[5] 2) within each apple harvesting zone, a second-stage optimal path planning is conducted by the TSP solution on individual apples. The above two stages of optimization form the HOPP algorithm in order to significantly reduce or minimize time cost in robotic apple harvesting. This work differentiates itself from other existing studies by contributing a new concept that 3D representation of apples can significantly enable and facilitate robotic apple harvesting and by contributing a novel HOPP algorithm.

Methods

3D environment setup:

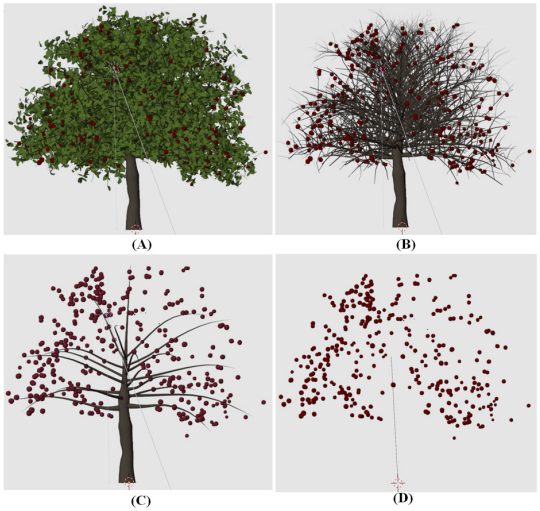

Figure 1: Illustration of the 3D model of an apple tree and its apples. (A) Full 3D model of the apple tree. (B) Leaves are removed from the tree. (C) Small branches are removed further. (D) Trunk is removed further and only apples are kept.

This work uses a commercially purchased realistic 3D model of apple trees (from TurboSquid website) that includes 349 apples on it (represented in obj file format). Specifically, the apple tree's 3D model includes 640,768 vertices and 458,022 faces. Figure 1 illustrates several views of the apple tree and its apples. All of the HOPP algorithm developments and evaluations in this work are based on the 3D model in Figure 1. According to the 3D rendering of apples, it is observed that spatial distributions of apples are quite irregular, e.g., some regions have higher apple densities, while other regions have lower apple densities. Therefore, a straightforward intuition is that such irregular spatial distribution of apples should be leveraged for optimal 3D path planning in robotic apple harvesting, that is, the apple harvesting robot should give higher priority to those regions with higher apple densities and plan its 3D path accordingly.

The HOPP algorithm:

Time cost is a key concern in robotic apple harvesting, e.g., the time costs of moving robotic shoulders and arms. In this work, I divided the total time cost of harvesting all apples into two stages: 1) moving the robotic shoulder across harvesting zones and 2) moving robotic arms to pick individual apples within each harvesting zone. Specifically, assume that the total number of robotic shoulder movements is $k-1$, that is, there are k harvesting zones, and each movement's average time cost is tshoulder. Then the total time cost of robotic shoulder movements is $(k-1)^*t_{shoulder}$. Within the workspace of robotic arms (e.g., simplified as a 3D sphere centered at the joint of robotic shoulder and robotic arms) in each harvesting zone, the average time cost for picking an individual apple when only moving the robotic arms is represented by tarm. Then, to pick all the apples (n) on a tree, the time needed for individual apple harvesting when moving the robotic arms is n^*t_{arm}. Therefore, the total time cost of harvesting all apples, including both robotic arm and shoulder movements, will be $(k-1)^*t_{shoulder}+ n^*t_{arm}$, which is the objective function of the HOPP algorithm to significantly reduce or minimize.

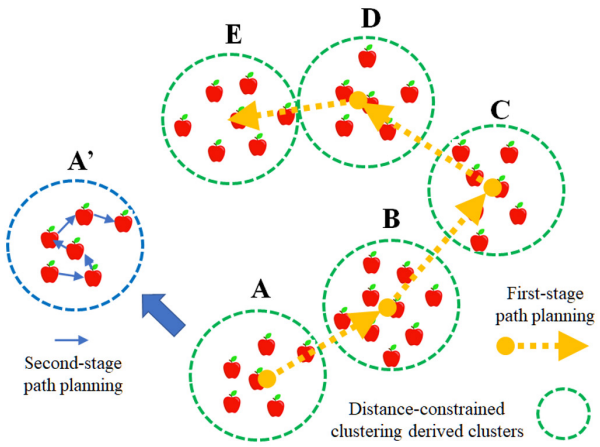

Figure 2: Overall idea of the HOPP algorithm. Here A-E represent five harvesting zones obtained by the distance-constrained *k*-means clustering. The path represented by orange arrows shows the first-stage optimal path across harvesting zones. The apples in A' are replicated from A. The blue arrows in A' show the second-stage optimal path across individual apples within a harvesting zone.

The overall idea of the 3D HOPP algorithm is simplified in a 2D space and illustrated in Figure 2. Specifically, in the first stage, all the apples will go through a distance-constrained k-means clustering so that these apples will be geographically grouped into neighboring harvesting zones (represented by the dashed green circles in Figure 2). Here, the harvesting robot arm's workspace is simplified by a circle. In the 3D case, the robotic arms can reach anywhere in the 3D spherical volume in the harvesting zone without the need of moving the robotic shoulder. Then, the optimal robotic path connecting those harvesting zones is formulated as the TSP and is solved using heuristic greedy search solutions, as illustrated by the dashed orange arrows (A->B->C->D->E) in Figure 2. Similarly, in the 3D case, the optimal path is obtained by connecting those 3D spheres via the TSP solution. Intuitively, the step of distance-constrained k-means clustering can minimize the total number of apple harvesting zones. That is, given the fixed diameter of robotic arms' spheric workspace, the distance-constrained *k-means* clustering can ensure that each grouped harvesting zone will include the largest possible number of apples, thus the total number of harvesting zones will be minimized. Also, the TSP solution to the cross-harvesting zone path can further minimize the average time cost of robotic shoulder movement. As a result, the total number

of robotic shoulder movements $k-1$ and each shoulder movement's average time cost is $t_{shoulder}$ are both minimized. Therefore, the total time cost of robotic shoulder movements $(k-1)^*t_{shoulder}$ is minimized.

In the second stage, within each apple harvesting zone, an optimal path planning is further conducted on individual apples by the TSP formulation and solution again, as illustrated in the dashed blue circle and blue arrows in A' on the left side of Figure 2. Therefore, the average time cost (t_{arm}) for picking an individual apple within each harvesting zone is minimized, and the total time needed for harvesting all individual apples (n^*t_{arm}) when moving robotic arms is minimized. Thus, through the HOPP algorithm, the total time cost of harvesting all apples ($(k-1)^*t_{shoulder} + n^*t_{arm}$), including time costs for both robotic arm and shoulder movements, is minimized.

Distance-constrained k-means clustering for grouping apples into harvesting zones:

Data clustering is a commonly employed methodology to group or partition a set of observational data (e.g., apples in this work) into collections with small within-group distances (e.g., within each apple harvesting zone) and big cross-group distances (e.g., across apple harvesting zones). Among various data clustering methodologies, one of the most popular methods is the k–means clustering algorithm.[6] Briefly, the k-means clustering algorithm utilizes iterative refinement to generate a data clustering result after taking the number of clusters k and the dataset (e.g., apples' spatial coordinates in this work) as the input. The k-means clustering algorithm starts with an initial estimate for the k centroids, which can either be randomly created or randomly selected from the dataset. The algorithm then iterates between two steps of data assignment and centroid update. More specifically, in the data assignment step, each centroid defines one cluster, and each data point is assigned to its nearest centroid based on the metric of Euclidean distance, e.g., distance between apples' spatial coordinates in this work. In the centroid update step, the cluster centroids are recomputed and updated by averaging the coordinates of all data points (e.g., apples' spatial coordinates here) that are assigned to that centroid's cluster. The k-means clustering algorithm iterates between the above two steps until a stopping criterion is met, i.e., no data points change clusters, the sum of the distances is minimized, or a maximum number of iterations is performed.

However, in this work's context, directly applying the k-mean clustering algorithm to the apples' data points would not work well due to the following reasons. First, it will be challenging to determine the right selection of cluster number k in our application scenario if the k-means clustering algorithm is directly applied. Second, it is hard to satisfy that the derived clusters will form valid apple harvesting zones, that is, all apples within a harvesting zone can be reached by the robotic arms, meaning that the distance between any apple and the centroid of the harvesting zone is shorter than the maximum length of the robotic arms. Therefore, a modified variant of k-mean clustering is adopted in this work's context, that is, the distance-constrained k-mean clustering.[4]

Mathematically, the following problem definition of distance-constrained k-mean clustering is adopted. Consider a collection of n apples' 3D coordinate data, $x1,\ldots,xn$, with $xi \in R^3$, I aim to select a number of k groups or clusters (harvesting zones), $C1,\ldots,Ck$. It typically holds that $k \ll n$. Each cluster Cj is assigned with a cluster centroid $cj \in R^3$, which represents the center that apple cluster. An apple $xi \in R^3$ is said to belong to cluster Cj if its distance from the centroid ch, with $h \neq j$, of every other cluster Ch is larger than its distance from Cj. If xi belongs to Cj, I set a binary assignment variable $ri, j \in B$ to 1, and to 0 otherwise. The solution of the apple clustering problem with distance constraint involves the computation of the optimal choice of cluster centroids cj, for $j=1,\ldots,k$, that minimizes the total of the distance of every apple xi from the cluster it belongs to. More specifically, the problem is defined as follows.

I aim to find a choice of k, of the cluster centroids, $cj \in R^3$, and measurement data assignments, $ri, j \in B$, that minimizes the objective function E:

$$E = \sum_{i=1}^{n} \sum_{j=1}^{k} ri,j * \|xi - cj\| \quad (1)$$

Subject to the following three constraints:

$$\text{I: } \sum_{j=1}^{k} rij = 1, \ \forall i = 1, \ldots, n \quad (2)$$

$$\text{II: } \|xi - cj\| \leq \beta/2, \ \forall i = 1, \ldots, n; \ \forall j = 1, \ldots, k \quad (3)$$

$$\text{III: } rij \in \{0,1\}, \ \forall i = 1, \ldots, n; \ \forall j = 1, \ldots, k \quad (4)$$

The first constraint (I) along with the third one (III) implies that each apple is assigned exactly to one cluster (harvesting zone); the constraints (II) imply that β is the diameter of the harvesting zone and the distance between any apple in this harvesting zone and its centroid is less than or equal to its radius; finally, constraints (III) imply that rij are binary decision variables.

The definitions in Equations (1)-(4) fit our apple harvesting zone definition (illustrated in Figure 2) very well. Notably, in the literature, the constraint (II) in Equation (3) has not been considered, as far as I know. Including such a constraint, however, is quite useful in this work, since it will ensure the HOPP algorithm's ability to define valid apple harvesting zones within a predefined spherical robotic arm workspace. Meanwhile, the objective function in Equation (1) ensures that the total number of apple harvesting zones is minimized. To find a plausible solution to the problem defined in Equations (1)-(4), the method that used a Hegelsmann-Krause (HK) model was adopted in this work to find an appropriate k first before the distance-constrained k-means clustering.[4,7] The core idea of the HK model is that data points with completely different attributes (e.g., geometric distances here) do not influence each other, while some sort of mediation occurs among data points whose distances are close enough.[7] It has been justified and demonstrated that the HK model is well suited for the distance-constrained k-means cluster.[4]

Traveling salesman problem solution and hierarchical optimal 3D path planning :

Once the apples have been clustered into harvesting zones via the methods in Equations (1)-(4), the spatial relationships among neighboring harvesting zones can be represented by a

DOI: 10.36838/v4i4.6

graph, e.g., spatially adjacent harvesting zones are linked by an edge, as illustrated in Figure 2. Then, the optimal 3D path planning at the first stage of harvesting zone is formulated as a TSP and solved using existing solution.[5] Theoretically, TSP is an NP-hard problem in combinatorial optimization and a heuristic greedy search algorithm is typically employed to obtain a near optimal result. Notably, the TSP formulation and solution has been utilized in many path planning problems in agriculture robotics and automation. Here, a heuristic greedy search implementation of TSP problem was adopted to find the optimal path given the clustered apple harvesting zones and their neighborhood graph, as illustrated in Figure 2. Thus, both the total number of robotic shoulder movements k and each shoulder movement's average time cost is $t_{shoulder}$ are minimized via the distance-constrained k-means clustering of apples and the TSP solution of optimal path planning at the harvesting zone level, respectively. Through this first stage of optimal 3D path planning, the total time cost of robotic shoulder movements $(k-1)*t_{shoulder}$ is thus minimized.

Similarly, in the second stage of path planning, an optimal path search is further conducted on individual apples by the TSP formulation and solution again, as illustrated by the apples in A' of Figure 2. As a result, the average time cost t_{arm}) for picking an individual apple within each harvesting zone is minimized, and thus the total time cost for harvesting all individual apples ($n*t_{arm}$) is minimized. Finally, the two-stage HOPP algorithm is summarized in Figure 3.

Input: n apples, represented by xi $(i=1,...,n)$

Stage 1: distance-constrained k-means clustering of xi $(i=1,...,n)$ into k apple harvesting zones.

The Hegelsmann - Krause (HK) model is used to determine the best k clusters.

The robot arm workspace's sphere diameter β is used to constrain the size of each harvesting zone (Equation (2)).

The distance-constrained k-means clustering algorithm is used to group all apples into k harvesting zones (Equations (1)-(4)).

Use TSP formulation and heuristic search solution to find the 3D optimal path across k harvesting zones.

This stage achieves the minimization of the total time cost of robotic shoulder movements ($(k-1)*t_{shoulder}$).

Stage 2: Use TSP formulation and solution to find the 3D optimal path within each harvesting zone.

The stage achieves the minimization of individual apple harvesting ($n*t_{arm}$).

Output: hierarchical optimal 3D path across all harvesting zones and individual apples.

Figure 3: Summary of the two-stage HOPP algorithm for robotic apple harvesting. Details of each stage or step have been provided in the above sub-sections.

Results and Discussion

Experiments:

A series of experiments were designed and conducted to demonstrate the effectiveness and performance of the proposed HOPP algorithm summarized in Figure 3 and detailed in the above sections. The 3D models of apples in Figure 1 were used in these experiments.

As explained in Equation (3) and summarized in Figure 3, the parameter β describes the diameter of apple harvesting robot arms' spherical workspace and it is a key factor that decides the output of the distance-constrained k-means clustering algorithm (Equations (1)-(4)). By alternating different β values, various apple harvesting zone clustering results were obtained by the HOPP algorithm. For quantitative comparison, a traditional path planning method (named Method 2 here) was considered as follows. It randomly selects apples to start with the harvesting process and uses greedy search in a local neighborhood for path planning. That is, Method 2 always goes from the current apple to the next neighbor with the shortest distance. Again, the average time cost for picking an individual apple within each harvesting zone is represented by t_{arm}, and each shoulder movement's average time cost is $t_{shoulder}$. Then, I compare the total time costs for both path planning methods (HOPP and Method 2), that is, $(k-1)*t_{shoulder} + n*t_{arm}$. Here, it is assumed that the time cost $t_{shoulder}$ is proportional to the distance between two harvesting zones (either minimized by the TSP optimization in HOPP or not in Method 2), and that the time cost t_{arm} is proportional to the distance between two individual apples (either minimized by the TSP optimization by HOPP or by greedy search in Method 2). It turned out that the time costs t_{arm} and $n*t_{arm}$ are quite close for HOPP and Method 2 as both methods employed a greedy search process among neighboring individual apples. Therefore, the following experimental comparisons focus on the time costs of robotic shoulder movements $(k-1)*t_{shoulder}$.

When β=1.75 (based on the distance unit in the 3D model of apple tree in Figure 1), 16 apple harvesting zones were obtained by the HOPP method, as shown by the large color spheres in Figure 4A. The derived optimal 3D optimal path is represented and visualized by the white lines in Figure 4A and by the corresponding blue arrows Figure 4B. It is apparent in Figure 4A that each clustered harvesting zone exhibits high density of apples, meaning that each robotic shoulder movement can harvest as many apples as it can and therefore the time cost of robotic shoulder movement ($(k-1)*t_{shoulder}$) is minimized. Also, the optimal 3D path at the level of individual apples obtained by the TSP solution is represented by the white lines and shown in Figure 4C. In comparison, the path planning results by Method 2 are shown in Figures 4D-4F in a similar way. It is interesting that the planned path by Method 2 takes 40 robotic shoulder movements (for one random run) from one harvesting zone to another. That is, without taking advantage of global distribution of all apples and without the distance-constrained k-means clustering, the planned path by Method 2 takes 2.67 times the robotic shoulder movements (40 steps) to harvest all apples when compared to the HOPP method (15 steps). This result apparently suggests the effectiveness of the proposed HOPP method and the importance of taking the advantage of the global information of spatial distributions of all apples on trees for more efficient apple harvesting.

Notably, Method 2 randomly selected the start apple to harvest and thus its total steps of robotic shoulder movements is random. I repeated Method 2 30 times and the statistical results are shown in Figure 5. On average, the planned path by Method 2 takes 2.85 times the robotic shoulder movements (42.73 steps) to harvest all apples than the HOPP method (15 steps), as shown in Figure 5A. Also, the average path distances

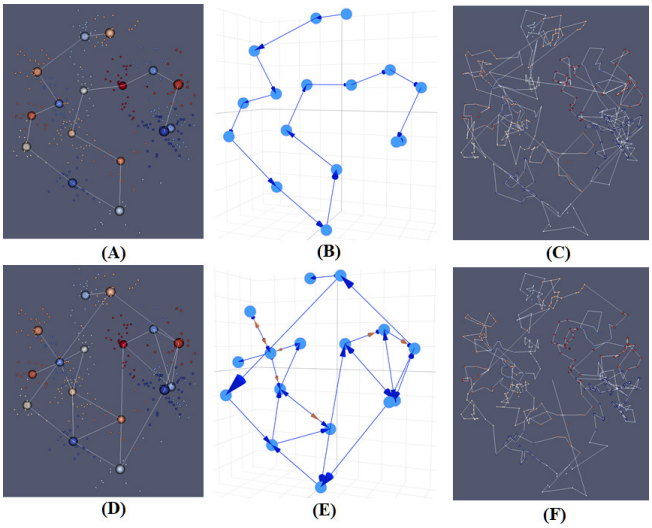

Figure 4: (A)-(C): visualization of result by HOPP. (A) The small spheres represent apples, and each color represents one harvesting zone. The large spheres are the centers of clustered harvesting zones, and their colors correspond to the apple clusters. The white lines are the path across harvesting zones. (B) The harvesting zone path in (A) is represented by blue arrows with directions. (C) Harvesting path at individual apple level. Each while line represents one step. The apple colors represent the clusters in (A). (D)-(F): The visualization of results by Method 2. In (E), for some pairs of harvesting zones, there are multiple path steps, and they are represented by multiple color arrows (blue and brown).

across harvesting zones by Method 2 (111.80) are 3.06 times more than the HOPP method (36.49), as shown in Figure 5B. Therefore, in terms of $(k-1)*t_{shoulder}$, Method 2 takes 8.72 times the harvesting time by the HOPP method.

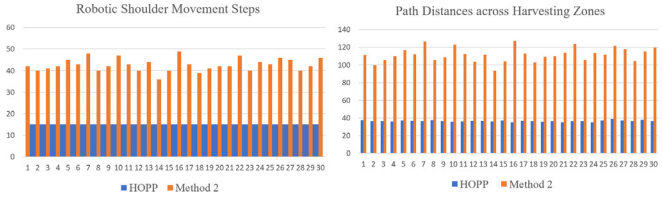

Figure 5: Comparison of HOPP and Method 2. Both methods were run for 30 times. (A) The total number of robotic shoulder movement steps in all 30 runs. The average steps for HOPP and Method 2 are 15 and 42.73, respectively. (B) Path distances across harvesting zones in 30 runs. It is noted that the initial position of HOPP slightly impacts its result. The average distances for HOPP and Method 2 are 36.49 and 111.80, respectively.

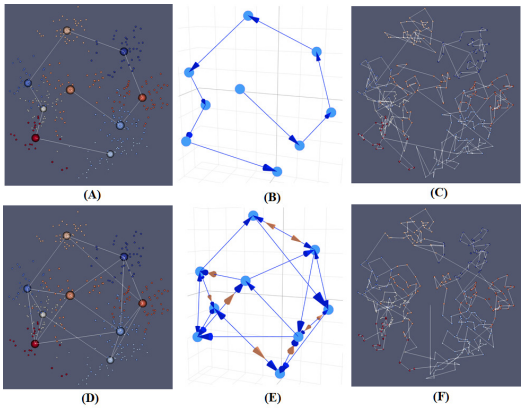

Figure 6: (A)-(C): visualization for HOPP. (A) The small spheres represent apples, and each color represents one harvesting zone. The large spheres are the centers of clustered harvesting zones, and their colors correspond to the apple clusters. The white lines are the path across harvesting zones. (B) The harvesting zone path in (A) is represented by blue arrows with directions. (C) Harvesting path at individual apple level. Each while line represents one step. The apple colors represent the clusters in (A). (D)-(F): The visualization results for Method 2. In (E), for some pairs of harvesting zones, there are multiple path steps, and they are represented by multiple color arrows (blue and brown).

When β=2.2, 9 apple harvesting zones were obtained by the HOPP method (Figures 6A-6B), and the optimal 3D optimal path is shown in Figure 6C. The path planning for Method 2 is shown in Figures 6D-6F. It is clear in Figure 6 that the proposed HOPP method takes significantly less time than Method 2. Again, Method 2 randomly selected the start apple to harvest and thus its total steps of robotic shoulder movements is random. I repeated the Method 2 for 30 times and the statistical results are shown in Figure 7. On average, the planned path by Method 2 takes 4.23 times the robotic shoulder movements (33.90 steps) to harvest all apples than that of the HOPP method (8 steps), as shown in Figure 7A. Also, the average path distances across harvesting zones by Method 2 (111.93) are 4.76 times more than those by the HOPP method (23.51), as shown in Figure 7B. Therefore, in terms of $(k-1)*t$-shoulder, Method 2 takes 20.13 times more harvesting time than the HOPP method.

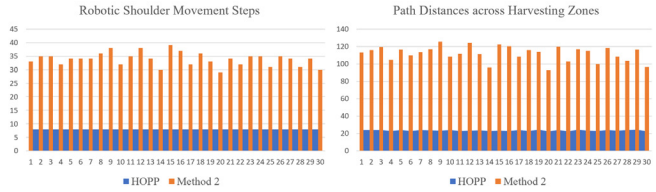

Figure 7: Comparison of HOPP and Method 2. Both methods were run for 30 times. (A) The total number of robotic shoulder movement steps in all 30 runs. The average steps for HOPP and Method 2 are 8 and 33.90, respectively. (B) Path distances across harvesting zones in 30 runs. The average distances for HOPP and Method 2 are 23.51 and 111.93, respectively.

Reconstruction of 3D apple tree model:

Following the direction of 3D path planning for robotic apple harvesting and inspired by existing efforts of 3D reconstruction from image sequences,[8] an initial effort was made to reconstruct 3D apple tree model in a lab environment. As shown in Figure 8, 63 photos (Figures 8A-8B) were taken around a laboratory apple tree by an iPhone from various angles and locations, and these photos were then used as the input for 3D reconstruction via the Meshroom software toolkit.[9] The Live Reconstruction pane in Meshroom interface provides the visualization of each step in the 3D reconstruction, such as camera initialization and calibration, feature extraction, and structure from motion. Notably, the Meshroom toolkit utilizes a camera sensors database to determine the camera's internal parameters and group them together. Therefore, Meshroom can infer the rigid scene structure (3D points) with the pose (position and orientation) and internal calibration of all cameras (iPhone camera's different poses), as shown in Figure 8C. By using the calibrated cameras and the structure-from-motion step, Meshroom can generate a dense geometric surface of the 3D reconstruction of the apple tree, as shown in Figures 8C-8F. Although the 3D model's quality can be improved in the future, the experiment in Figure

DOI: 10.36838/v4i4.6

8 demonstrated the promise of reconstructing 3D models of apple trees using computer vision and computer graphics techniques. Given the rapid advancements of technologies, such as unmanned aerial vehicles (UAV) LiDAR or UAV camera data acquisition and 3D reconstruction,[10,11] it is predicted that robotic apple harvesting guided by 3D path planning will become practical in the future

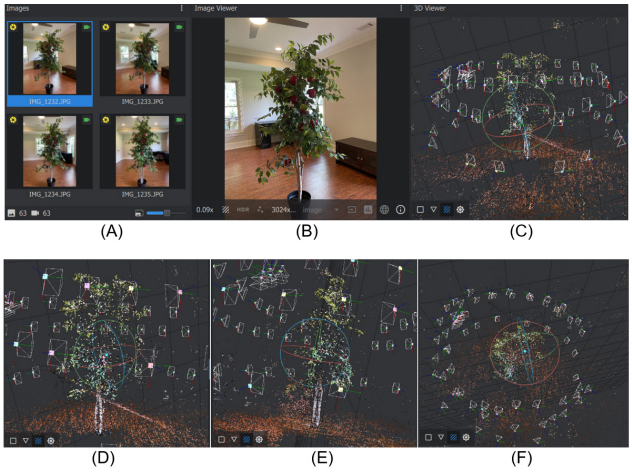

Figure 8: Reconstruction of 3D apple tree model. (A) Visualization of 63 images captured by iPhone camera from 63 poses. (B) Enlarged view of the first image in (A). (C) Reconstruction of the 3D apple tree model. (D)-(F): additional views of the 3D model in (C).

Path planning for fruit harvesting robotics:

From a general perspective of robotic path planning, the HOPP algorithm proposed in this paper belongs to off-line path planning,[12] that is, the apple harvesting robot has prior access to complete information about the 3D environment of apples and their tree. Meanwhile, this HOPP algorithm can be applied online during harvesting if more information (e.g., apple localization and 3D reconstruction) becomes available. Also, the HOPP algorithm belongs to the category of point-to-point path planning, that is, the goal consists of determining a path from a starting point to a destination point by optimizing key parameters such as time and distance.[12] The HOPP algorithm is akin to the general category of cell decomposition method in the robotic path planning domain, which decomposes the free space into small regions called cells (e.g., apple harvesting zones in this work) and then searches for an optimal path in the cell graph using algorithms such as A*, Dijkstra, or TSP.[12] The HOPP algorithm also shares similarities with the category of coverage path planning (CPP) algorithms, in that CPP is defined as the task of determining a path that passes overall points of an area or volume (e.g., apple harvesting zones here) while avoiding obstacles.[13] The HOPP algorithm and CPP share such common characteristics or requirements as the robot must cover the whole area (all apples), the robot should cover the entire region without overlapping, the robot should avoid all obstacles, the robot should use simple and smooth motion trajectories, and an optimal path is desired under considered criteria such as time and distance. However, it is not always possible to possess all these requirements or characteristics in complex agriculture environments like apple trees or orchards, and thus priority consideration is typically adopted. For instance, in its current form, the HOPP algorithm does not consider obstacle avoidance and does not plan robotic shoulder/arms motion trajectories.

There is much room to improve the HOPP algorithm in the future, such as considering obstacle avoidance, considering other optimization objectives like smoothness of robotic arms/shoulder movement, considering different time costs of robotic arm/shoulder movements, considering multiple simultaneous harvesting robots, and 3D path planning for harvesting many apple trees in the orchard. With these more complex considerations, the HOPP algorithm can be extended in various ways. For instance, the distance-constrained *k*-means clustering can be extended by adding additional obstacle avoidance into the optimization constraints, and the algorithm itself should be scaled to much larger number of apples like those in apple orchard. Also, the TSP formation and solution for finding the optimal path can be extended into a multiple TSP (mTSP) formation if there are several apple harvesting robots simultaneously participating in the apple picking.

It is known that the k-means clustering algorithm has a time complexity of $O(n^2)$, where n is the input data size. This quadratic complexity debars the algorithm from being effectively used in large-scale applications. Researchers have explored lower-complexity implementation of the *k*-means clustering algorithm, such as the $O(n)$ complexity (linear order) counterpart of the *k*-means.[14] In the future, such lower-complexity implementation could be employed into the HOPP algorithm for apple harvesting zone clustering via distance-constrained k-means clustering, which is the most time-consuming part of the 3D path planning algorithm. Also, such lower-complexity heuristic search algorithms can be explored for the TSP and mTSP solutions once the harvesting zones are mapped. These lower-complexity implementation of the 3D path planning algorithm is quite important for online path planning in large-scale apple harvesting in real-world orchards. Finally, this work does not provide a theoretical analysis of the algorithmic aspect of the HOPP method, which should be investigated in the future.

■ Conclusion

The world's population is projected to reach nine billion people by the year 2050, which suggests that agricultural productivity must increase substantially and sustainably. The automatization of agricultural tasks, including fruit harvesting, is an essential step to deal with population growth. Various types of agricultural robots have been explored in the past few decades, however, how to deal with the unstructured agricultural environment is one of the hardest challenges. This work proposes a conceptually new HOPP algorithm for robotic apple harvesting by decomposing the challenging task into two-stage hierarchical apple harvesting zone clustering and optimal 3D path planning, and experimental results have demonstrated that the HOPP algorithm can gain significant benefits, e.g., minimizing apple harvesting time cost. In addition to the HOPP algorithm, another core contribution of this work is that it is demonstrated that the global information of spatial distributions of all apples should be leveraged for better apple harvesting. Although this proposed HOPP algorithm

leverages the availability of 3D models of apples at current stage, it is expected that reconstructing 3D structures of apples and their trees from UAVs equipped with camera, LiDAR or multispectral imaging sensors and enabled with advanced AI tools will become practical in the future. Also, despite that this work simplifies the apple tree environment and harvesting execution, the HOPP algorithm itself is scalable and extendable by including a variety of other considerations, such as obstacle avoidance and multiple harvesting robots, in the future.

Acknowledgements

I would like to thank Professor Charlie Li, Dr. Javier Rodriguez and Daniel Petti of Bio-Sensing and Instrumentation Lab, Phenomics and Plant Robotics Center, College of Engineering, University of Georgia, for their guidance and help when I performed an internship in their lab in Summer 2021 and Fall 2021. I would like to thank Zhengliang Liu and Jiaxing Gao for their guidance and help on data visualization and Python programming. I would like to thank my teacher Mike Callinan at Athens Academy who has been teaching me robotics courses and guiding me on robotics projects for over four years. Finally, I would like to thank my father for his guidance and support during my research.

References

1. Silwal, A.; Davidson, J. R.; Karkee, M; Mo, C.; Zhang, Q.; Lewis, K. Design, integration, and field evaluation of a robotic apple harvester, *J Field Robotics*. 2017, 34:1140-1159.
2. Jia, W.; Zhang, Y.; Lian, J.; Zheng, Y.; Zhao, D.; Li, C.; Apple harvesting robot under information technology: A review. *International Journal of Advanced Robotic Systems*. 2020, 17(3):1-16.
3. Tang, Y.; Chen, M.; Wang, C.; Luo, L.; Li, J.; Lian, G.; Zou, X. Recognition and Localization Methods for Vision-Based Fruit Picking Robots: *A Review, Front Plant Sci*. 2020, 11:510.
4. Oliva, G.; Manna, D. L.; Fagiolini, A.; Setola, R. Distance-constrained data clustering by combined k-means algorithms and opinion dynamics filters. *The 22nd Mediterranean Conference on Control and Automation*. 2014, pp. 612-619.
5. Held, M.; Karp, R.M. The Traveling Salesman Problem and Minimum Spanning Trees. *Operations Research*. 1970, 18(6):1138-1162.
6. Hartigan, J. A.; Wong, M. A. Algorithm AS 136: A k-means clustering algorithm. *Journal of the Royal Statistical Society, Series C*. 1979, 28(1):100-108..
7. Hegselmann, R.; Krause, U. Opinion dynamics and bounded confidence models, analysis, and simulation, *Journal of Artificial Societies and Social Simulation*. 2002, 5(3).
8. Qu, Y.; Huang, J.; Zhang, X.; Rapid 3D Reconstruction for Image Sequence Acquired from UAV Camera, *Sensors*. 2018, 18(1):225.
9. Kneip, L.; Scaramuzza, D.; Siegwart, R. A novel parametrization of the perspective-three-point problem for a direct computation of absolute camera position and orientation. *IEEE Computer Society Conference on Computer Vision and Pattern Recognition*. 2011, 2969-2976.
10. Hadas, E.; Jozkow, G.; Walicka, A.; Borkowski, A. Apple orchard inventory with a LiDAR equipped unmanned aerial system, *International Journal of Applied Earth Observation and Geoinformation*. 2019, 82:101911.
11. Chen. Y.; Zhang, B.; Zhou, J.; Wang, K. Real-time 3D unstructured environment reconstruction utilizing VR and Kinect-based immersive teleoperation for agricultural field robots, *Computers and Electronics in Agriculture*. 2020, 175:105579.
12. Mac, T. T.; Copot C.; Tran, D. T.; Keyser, R. D. Heuristic approaches in robot path planning: A survey, *Robotics and Autonomous Systems*. 2016, 86:13–28.
13. Galceran, E.; Carreras, M. A survey on coverage path planning for robotics, *Robotics and Autonomous systems*. 2013, 61(12):1258-1276.
14. Pakhira, M. K. A Linear Time-Complexity k-Means Algorithm Using Cluster Shifting, International Conference on Computational Intelligence and Communication Networks. 2014, pp. 1047-1051.

Author

David W Liu is a 10th grader in Athens Academy, Athens, GA. He is interested in robotics, computer programming, and mathematics. He has been taking robotics courses in Athens Academy since 6th grade and has been actively involved in multiple robotics activities such as FLL and FTC challenges since 6th grade.

DOI: 10.36838/v4i4.6